Biochemical and Biophysical Research Communications 449 (2014) 344–350

Contents lists available at ScienceDirect

Biochemical and Biophysical Research Communications

journal homepage: www.elsevier.com/locate/ybbrc

Schisantherin A suppresses osteoclast formation and wear particle-induced osteolysis via modulating RANKL signaling pathways

Yi He, Qing Zhang, Yi Shen, Xia Chen, Feng Zhou, Dan Peng *

Department of Orthopaedics, The Second Xiangya Hospital, Central South University, No.139 Middle Renmin Road, Changsha, Hunan 410011, PR China

ARTICLE INFO

Article history:
Received 20 April 2014
Available online 17 May 2014

Keywords:
Schisantherin A
Osteoclasts
RANKL
Osteolysis

ABSTRACT

Receptor activator of NF-κB ligand (RANKL) plays critical role in osteoclastogenesis. Targeting RANKL signaling pathways has been a promising strategy for treating osteoclast related bone diseases such as osteoporosis and aseptic prosthetic loosening. Schisantherin A (SA), a dibenzocyclooctadiene lignan isolated from the fruit of Schisandra sphenanthera, has been used as an antitussive, tonic, and sedative agent, but its effect on osteoclasts has been hitherto unknown. In the present study, SA was found to inhibit RANKL-induced osteoclast formation and bone resorption. The osteoclastic specific marker genes induced by RANKL including c-Src, SA inhibited OSCAR, cathepsin K and TRAP in a dose dependent manner. Further signal transduction studies revealed that SA down-regulate RANKL-induced nuclear factor-kappaB (NF-κB) signaling activation by suppressing the phosphorylation and degradation of IκBα, and subsequently preventing the NF-κB transcriptional activity. Moreover, SA also decreased the RANKL-induced MAPKs signaling pathway, including JNK and ERK1/2 posphorylation while had no obvious effects on p38 activation. Finally, SA suppressed the NF-κB and MAPKs subsequent gene expression of NFATc1 and c-Fos. In vivo studies, SA inhibited osteoclast function and exhibited bone protection effect in wear-particle-induced bone erosion model. Taken together, SA could attenuate osteoclast formation and wear particle-induced osteolysis by mediating RANKL signaling pathways. These data indicated that SA is a promising therapeutic natural compound for the treatment of osteoclast-related prosthesis loosening.

1. Introduction

Bone is a rigid yet dynamic organ. Osteoblast-induced bone formation and osteoclast-mediated bone resorption together maintain the metabolic balance. Disorders between osteoclasts and osteoblasts result in various skeletal diseases such as osteoporosis and osteopetrosis [1,2]. Osteoclasts are multinucleated cells differentiated from hematopoietic precursor cells of the monocyte/macrophage lineage [3]. Two primary cytokines, macrophage colony stimulation factor (M-CSF) and receptor activator of NF-κB ligand (RANKL) are critical in maintaining osteoclasts survival and differentiation. Specifically, M-CSF plays crucial role in the survival and proliferation of osteoclast precursors [4], while RANKL engages in the entire processes of osteoclasts differentiation and bone resorption [5].

Once upon the stimulation of RANKL, a member of the tumor necrosis factor (TNF) family cytokines [6] that interacts with the receptor RANK, tumor necrosis factor receptor (TNFR)-associated factors 6 (TRAF6) binds closely to the membrane [7,8] and evokes the activation of a series of cascades, such as nuclear factor κB (NF-κB) and mitogen-activated protein kinases (MAPKs) pathway [9–11], including extracellular signal-regulated kinase (ERK), c-Jun-N-terminal kinase (JNK), and p38 [12]. These signaling pathways ultimately lead to induction and activation of the nuclear factor of activated T cells c1 (NFATc1) [13], a master transcription factor for osteoclast differentiation [14,15].

To discover new types of anti-resorptive agents, we screened for natural compounds that regulate osteoclast differentiation. In our screening, we have found that Schisantherin A has strong inhibitory effects on osteoclast formation in vitro. Schisantherin A, a dibenzocyclooctadiene lignan isolated from the fruit of Schisandra sphenanthera, has been used as an antitussive, tonic, and sedative agent under the name of Wuweizi in Chinese traditional medicine [16]. However, its beneficial effects on bone metabolism have not previously been evaluated. In the present study, we investigated

* Corresponding author.
E-mail address: xyeypd@163.com (D. Peng).

http://dx.doi.org/10.1016/j.bbrc.2014.05.034
0006-291X/

the effects of SA on osteoclast differentiation and function, RANKL-induced signaling pathways, and bone resorption in an in vivo model.

2. Materials and methods

2.1. Media and reagents

Schisantherin A was purchased from Shanghai Haoran Biologic Technology Co., Ltd (Shanghai, China). Dulbecco's modified Eagle's medium (DMEM) and fetal bovine serum (FBS) were obtained from Invitrogen-Gibco (Grand Island, NY, USA). The Cell Counting Kit-8 (CCK-8) was obtained from Dojindo Molecular Technology (Japan). Soluble mouse recombinant macrophage colony-stimulating factor (M-CSF) and RANKL were purchased from Peprotech (USA). Tartrate-resistant acid phosphatase (TRAP) staining solution was from Sigma–Aldrich (St Louis, MO, USA). Phosphorylated-IκBα and MAPKs (anti-ERK1/2, anti-JNK, and anti-p38) mouse or rabbit antibodies were purchased from Cell Signaling Technology (Beverly, MA, USA).

2.2. Cell culture

Bone marrow-derived macrophages (BMMs) were harvested as previously described [17,18]. Generally, bone marrow cells were extracted from the femur or tibia of a 4-week-old C57/BL6 mouse and incubated in culture medium plus 30 ng/mL M-CSF. Wash the culture plates before replace medium to eliminate residual stromal cells. Harvest the adhered cells on the bottom of the dish as BMMs. The complete cell culture medium was DMEM with 10% FBS, penicillin (100 units/mL), and streptomycin (100 μg/mL). The cells were maintained in a humidified atmosphere of 95% air and 5% CO_2 at 37 °C.

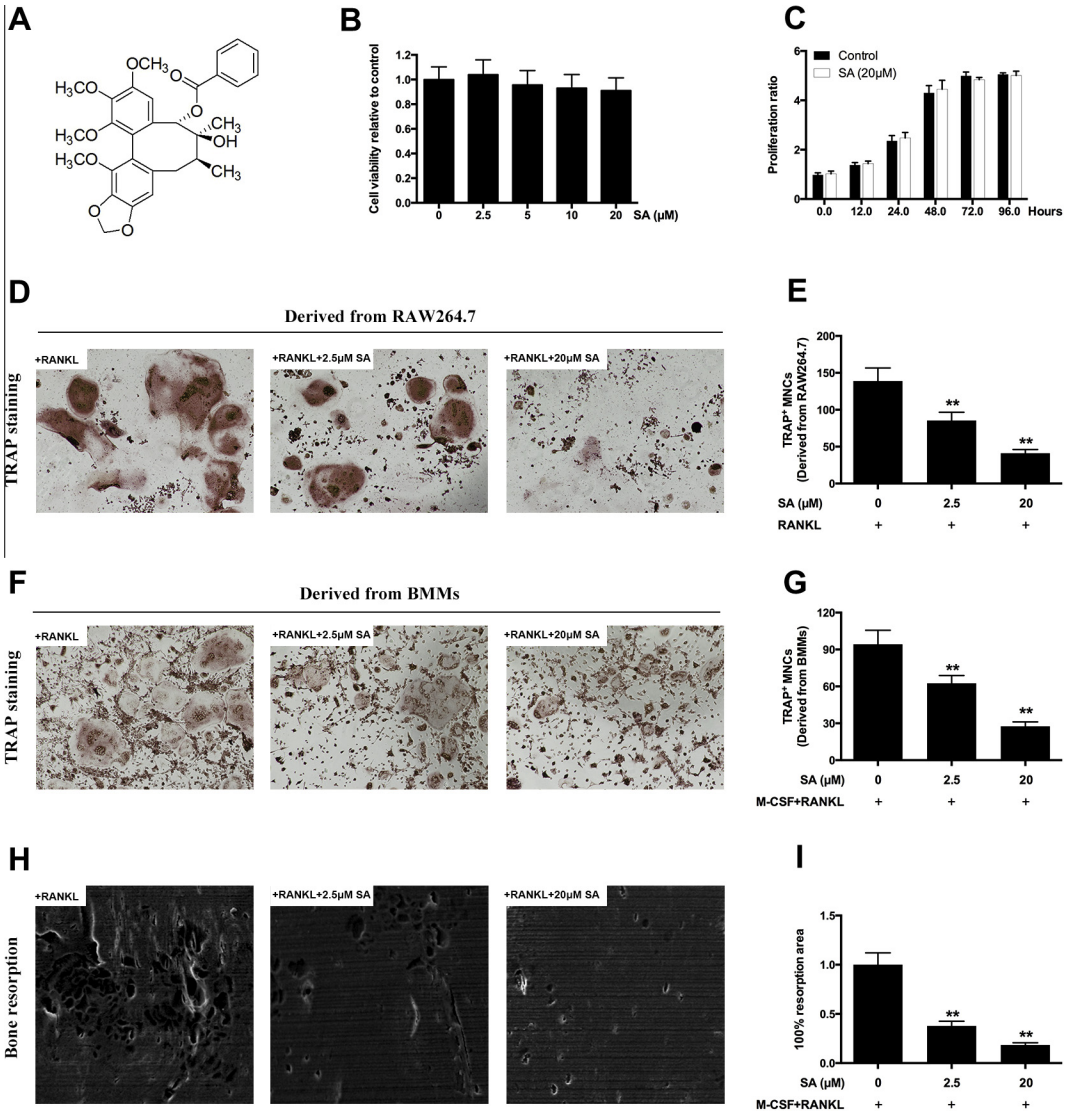

Fig. 1. SA inhibited RANKL-induced osteoclast formation and function in a dose-dependent manner without cytotoxicity. (A) Structure of SA. (B) BMMs were treated with various concentrations of SA for 48 h, and cell viability was measured by using the CCK8 assay. (C) BMMs were treated with 20 μM SA for the indicated times, and cell viability was measured by using the CCK8 assay. (D) RAW264.7 cells were treated with various concentrations of SA followed by RANKL (100 ng/mL) stimulation for 5 days. Then, cells were subjected to TRAP staining. (E) Multinucleated osteoclasts were counted. (F) BMMs were treated with various concentrations of SA followed by M-CSF (30 ng/mL) and RANKL (100 ng/mL) stimulation for 5 days. Then, cells were subjected to TRAP staining. (G) Multinucleated osteoclasts were counted. (H) BMMs were plated on bone slices and cultured with or without M-CSF (30 ng/mL) and RANKL (100 ng/mL). Four days later, cells were cultured in the presence of the indicated concentrations of SA for another four days. Bone resorption pits on bone slices were then examined by scanning electron microscopy. (I) The bone resorptive pit areas formed by osteoclasts were analyzed and processed using the Image pro-plus system. Resorptive areas are expressed as mean ± SD. $^{*}p < 0.05$ and $^{**}p < 0.01$ versus controls.

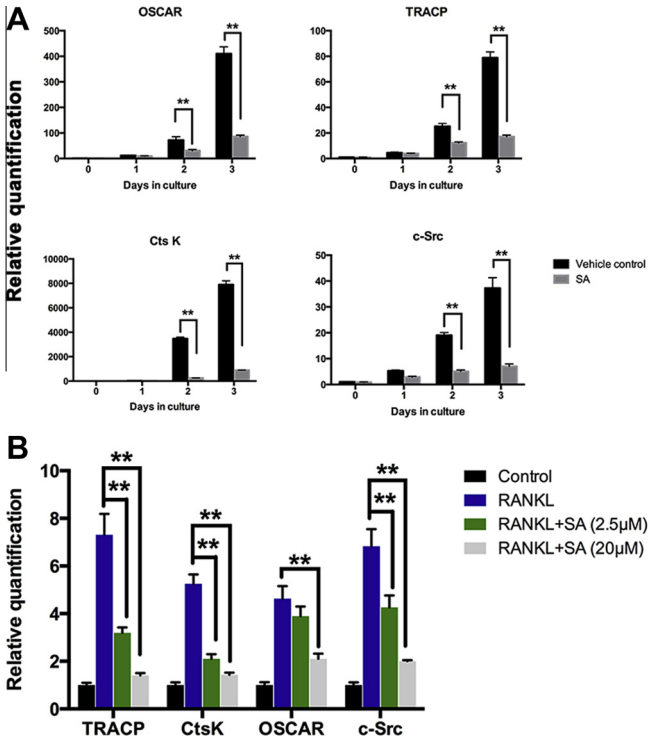

Fig. 2. SA suppresses RANKL-induced osteoclast specific gene expression. (A) BMMs were cultured with or without M-CSF (30 ng/mL), RANKL (100 ng/mL) and 20 μM SA for 0, 1, 2 or 3 days. RANKL-induced gene expression was detected by real-time PCR assay. (B) BMMs were cultured with M-CSF (30 ng/mL), RANKL (100 ng/mL) and indicated concentrations of SA. RANKL-induced gene expression was detected by real-time PCR assay. Expression levels were normalized relative to the expression of β-actin. The results are expressed as mean ± SD. $^{*}p < 0.05$ and $^{**}p < 0.01$ versus controls.

2.3. Cell viability assay

The effect of SA on cell viability of BMMs and RAW264.7 cells was detected via the Cell Counting Kit-8 (CCK-8; Dojindo Laboratories, Kumamoto, Japan). Briefly, cells were pretreated with indicated doses of SA for 48 h, or with indicated days under 20 μM SA, followed by addition of 10 μL CCK-8 solution to each well. After 4 h incubation, absorbance was measured at 450 nm using a microplate reader. The effect of SA on cell viability was expressed as percent cell viability, with vehicle-treated control cells set at 100%.

2.4. In vitro osteoclastogenesis assay

In vitro osteoclastogenesis assays were preformed to examine the effects of SA on osteoclast differentiation from both BMMs and raw264.7 cell line. BMMs were plated in the 96-well plates at a density of 6×10^3 cells/well in triplicate and treated with various concentrations of SA (0, 2.5, or 20 μM) plus M-CSF (30 ng/mL) and RANKL (100 ng/mL). Meanwhile, raw264.7 cells were plated in the 96-well plates at a density of 2×10^3 cells/well in triplicate and treated with various concentrations of SA (0, 2.5, or 20 μM) plus RANKL (100 ng/mL). After five days, cells were fixed and stained for TRAP activity. TRAP+ multinucleated cells with more than five nuclei were counted as osteoclasts.

2.5. Bone resorption assay

For bone resorption assay, BMMs at 6×10^3 cells/well were seeded on bone slices in 96-well plates and stimulated with M-CSF (30 ng/mL) and RANKL (100 ng/mL). Four days later, pre-osteoclasts were treated with various concentrations of SA for another four days. Bone slices were then fixed with 2.5% glutaraldehyde and imaged using a scanning electron microscope (SEM; FEI Quanta 250). Pit areas were quantified and analyzed. The experiments were repeated at least three times.

2.6. Real-time polymerase chain reaction analysis

Total RNA was extracted from BMMs by using the RNeasy Mini Kit (Qiagen, Valencia, CA, USA). cDNA was synthesized from total RNA using reverse transcriptase (TaKaRa Biotechnology, Otsu, Japan), and amplified using polymerase chain reaction (PCR). Real-time PCR was performed using the SYBR Premix Ex Tag kit (TaKaRa Biotechnology) and the ABI 7500 Sequencing Detection System (Applied Biosystems, Foster City, CA, USA). The detector was programmed with the following PCR conditions: 40 cycles of 5-s denaturation at 95 °C and 34-s amplification at 60 °C. All reactions were run in triplicate and were normalized to the housekeeping gene β-actin. Primers for osteoclastogenic genes used in this study were as follows: mouse β-actin: forward, 5′-tttgatgtcacgcacgatttcc-3′ and reverse, 5′-tgtgatggtgggaatgggtcag-3′; mouse TRAP: forward, 5′-ctggagtgcacgatgccagcgaca-3′ and reverse, 5′-tccgtctcggcgatggaccaga-3′; mouse CTSK: forward, 5′-cttccaatacgtgcagcaga-3′ and reverse, 5′-acgcaccaatatcttgcacc-3′; mouse OSCAR: forward, 5′-agggaaacctcatccgtttg-3′ and reverse, 5′-gagccggaaataaggcacag-3′; mouse c-Src: forward, 5′-ccaggctgaggagtggtact-3′ and reverse, 5′-cagcttgcggatcttgtagt-3′; mouse NFATc1: forward, 5′-ccgttgcttccagaaaataaca-3′ and reverse, 5′-tgtgggatgtgaactcggaa-3′.

2.7. Western blot analysis

Cells treated for the indicated time with various concentrations of SA were washed with cold PBS and lysed with RIPA buffer plus PMSF. Cell lysates were centrifuged at 12,000 rpm for 10 min, and supernatants were collected as samples. Protein (30 μg) was separated on 10% SDS–PAGE and transferred to PVDF membranes. The membranes were blocked with 5% skim milk in TBST containing 0.05% Tween-20 and probed successively with mouse anti-phospho-IκBα, phospho-JNK, JNK, phospho-p38, p38, phospho-ERK, ERK, NFATc1 and β-actin overnight at 4 °C. Horseradish peroxidase-conjugated rabbit anti-mouse IgG antibodies were used as secondary antibodies for 1 h at room temperature. The signals were detected by exposure in an Odyssey infrared imaging system (LI-COR).

2.8. Luciferase reporter gene activity assay

The effect of SA on RANKL-induced NF-κB activation was measured using raw264.7 cells that had been stably transfected with an NF-κB luciferase reporter construct, as previously described [19,20]. Briefly, cells were seeded into 48-well plates and maintained in cell culture media for 24 h. Then, cells were pretreated with or without indicated concentrations of SA for 1 h followed by addition of RANKL (100 ng/mL) for 8 h. Luciferase activity was measured using the Promega Luciferase Assay System (Promega, Madison, WI, USA), and normalized to that of the vehicle control.

2.9. Calvarial osteolysis model and staining

All animal experiments were conducted in accordance with principles and procedures approved by the Central South University. A mouse calvaria model to determine the effects of Ti particle exposure was described previously [21]. Briefly, 12 healthy 6–8-weeks C57/BL6 mice were randomly assigned to two groups, Ti particles with PBS, and Ti particles with SA (30 mg kg^{-1} day^{-1}).

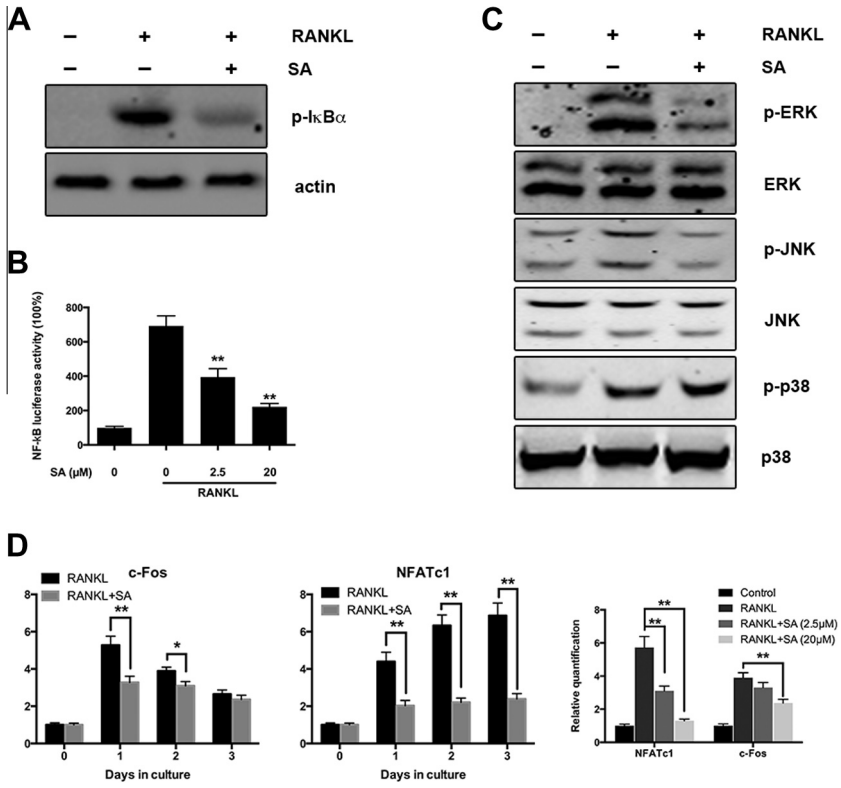

Fig. 3. SA blocks RANKL-induced activation of NF-κB and MAPKs (ERK/JNK) signaling pathways. (A) SA suppresses RANKL-induced IκBα phosphorylation and degradation. BMM cells were incubated with or without SA (20 μM) for 4 h and then treated with or without RANKL (100 ng/mL) for 10 min. Cell lysates were prepared for immunoblotting with antibodies as indicated. (B) SA inhibits RANKL-induced NF-κB-dependent luciferase reporter gene expression. After transfection of the NF-κB-luciferase reporter gene in RAW264.7 cells, the cells were incubated with the indicated concentrations of SA for 24 h and then stimulated with 100 ng/mL of RANKL for another 24 h. Cell supernatants were collected and assayed for luciferase activity as described in the Section 2. (C) SA inhibits the phosphorylation of MAPKs (JNK and ERK) induced by RANKL. BMM cells were incubated with or without SA (20 μM) for 4 h and then treated with or without RANKL (100 ng/mL) for 10 min. Cell lysates were prepared for immunoblotting with antibodies as indicated. (D) SA inhibits RANKL-induced c-Fos and NFATc1 expression. BMMs were cultured with M-CSF (30 ng/mL) and RANKL (100 ng/mL) at indicated concentrations and time of SA. RANKL-induced gene expression was detected by real-time PCR. Expression levels were normalized relative to the expression of β-actin. The results are expressed as mean ± SD. $^{*}p < 0.05$ and $^{**}p < 0.01$ versus controls.

The mice were anesthetized, the cranial periosteum was separated from the calvarium by sharp dissection, and 3 mg of Ti particles were placed directly on the surface of the bone. Mice in the Ti SA group were injected intraperitoneally with SA 30 mg kg^{-1} day^{-1} for 10 days. Mice in the Ti PBS group received PBS daily. At the end of treatment the mice were killed and the calvaria excised, fixed with 4% formaldehyde overnight, and then the calvaria were decalcified in EDTA and histological sections were prepared, followed by staining with hematoxylin and eosin (H&E), and TRAP stain (Sigma) according to the manufacturer's instructions.

2.10. Statistical analysis

All values are presented as the mean ± standard deviation (SD) of the values obtained from three or more experiments. Statistical significances were determined by Student's *t*-test. A value of $p < 0.05$ was considered significant.

3. Results

3.1. Effect of SA on cell viability

BMMs cells were treated with various concentrations of SA for 48 h, and cell viability was assessed with the CCK-8 assay kit. SA had no cytotoxic effects on BMMs at concentrations less than 20 μM compared with the control treatment (Fig. 1B). Furthermore, 20 μM SA was chosen for subsequent cytotoxic analysis for longer periods. As shown in Fig. 1C, during the whole culture period of four days, SA had no inhibitory effect on BMM proliferation. The same effect of SA on raw264.7 cells viability was also detected (data not shown here).

3.2. Effect of SA on osteoclast differentiation in RANKL-stimulated BMMs and RAW264.7 cells

To determine the effect of SA on osteoclast differentiation, we treated both primary BMMs and raw264.7 cells with various concentrations of SA in the presence of RANKL. Mature multinucleated TRAP-positive osteoclasts were seen in RANKL group. However, SA greatly retarded osteoclast differentiation from both primary BMMs and raw264.7 cells in a dose-dependent manner (Fig. 1D–G). These data suggest that SA effectively suppresses number of osteoclasts, and that SA may be a potent inhibitor of osteoclastogenesis.

3.3. Effect of SA on osteoclastic bone resorption in vitro

We next investigated whether SA could inhibit osteoclastic bone resorption in vitro. Osteoclast precursors were plated on bone slices and treated with the indicated concentrations of SA. As shown in Fig. 1H, bone resorption area substantially reduced in the SA-treated group. Osteoclastic bone resorption was almost completely abrogated after treatment with 20 μM SA (Fig. 1I). Collectively, these findings suggested that SA impaired osteoclast bone resorption in vitro.

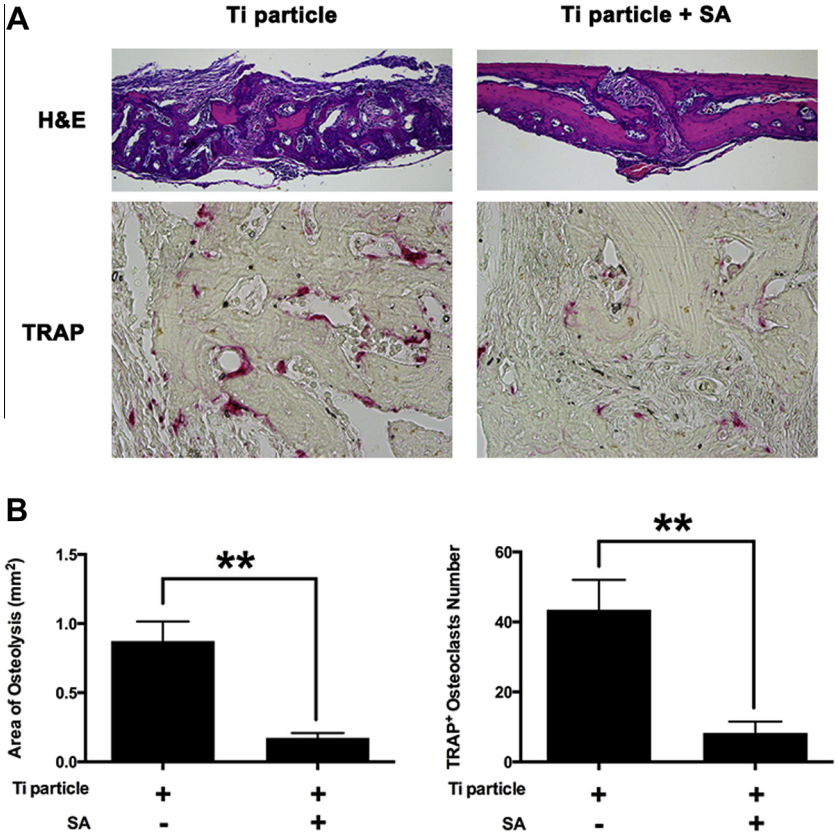

Fig. 4. SA prevented Ti particle-induced osteolysis by inhibiting osteoclast activity. (A) Calvaria were fixed, decalcified, dehydrated, embedded, and sectioned. Sections were stained with H&E and TRAP. (B) Area of osteolysis (mm^2), and (C) Number of osteoclasts were analyzed. Asterisks indicate statistically significant differences ($^{*}p < 0.05$; $^{**}p < 0.01$) between groups.

3.4. SA suppressed osteoclastic gene expression in vitro

To further confirm the inhibitory effect of SA on osteoclast differentiation, osteoclastic gene expression profile was investigated. As shown in Fig. 2A, the expression of osteoclastic specific genes was gradually induced during osteoclastogenesis, including TRAP, Cts K, OSCAR, and c-Src. However, the induction of these genes was suppressed dramatically by the presence of SA. In addition, we further confirmed that SA dose-dependently suppressed osteoclast differentiation, evidenced by the suppression of these osteoclast specific genes at 2.5 μM and 20 μM respectively (Fig. 2B). Collectively, these data supported the inhibition on osteoclast formation by SA.

3.5. Effect of SA on NF-κB and MAPKs activation

The activation of NF-κB is critical for RANKL-induced osteoclastogenesis [22]. NF-κB is inactive in the cytosol because it is bound to IκB, and becomes active after IκB has been phosphorylated and subsequently degraded [23]. Thus, we investigated whether SA inhibits phosphorylation and degradation of IκB. Accordingly, BMMs were pretreated for 4 h with SA, and phosphorylated-IκBα protein levels were determined after 10 min of further exposure to RANKL (100 ng/mL). SA was found to significantly suppress RANKL-induced phosphorylation and degradation of IκBα (Fig. 3A). Furthermore, the inhibitory effects of SA on NF-κB activation were further supported by luciferase assays. The transcriptional activity of NF-κB increased dramatically following treatment with RANKL. However, SA inhibited NF-κB activity in a concentration-dependent manner (Fig. 3B).

Besides the NF-κB signaling pathway, activation of the MAPKs pathway plays a pivotal role in osteoclastogenesis [19,24]. To evaluate the effects of SA on MAPKs following the stimulation of RANKL in BMMs, we examined the phosphorylation of p38, JNK, and ERK by western blot analysis. Our results showed that SA significantly inhibited RANKL-induced phosphorylation of JNK and ERK, while had no inhibitory effect on p38 phosphorylation (Fig. 3C). These results indicated that SA could inhibit RANKL-induced activation of MAPKs in osteoclasts.

3.6. Effects of SA on RANKL-induced NFATc1 expression

NFATc1 is a well-known master regulator of osteoclastogenesis and osteoclast function [25]. NF-κB and MAPK pathways are the two main activators that can regulate the NFATc1 promoter and NFATc1 expression [19,26]. NF-κB induces the initial induction of NFATc1, the expression of which is auto-amplified by NFATc1 binding to its own promoter in cooperation with c-Fos [27,28]. To determine whether SA regulates the expression of NFATc1 by inhibiting the NF-κB and MAPK signaling pathways, we examined the expression of c-Fos and NFATc1 at the mRNA level. Both c-Fos and NFATc1 were increased when cells were exposed to RANKL, whereas SA abrogated the RANKL-induced increases in c-Fos and NFATc1 at the mRNA level throughout the experimental period (Fig. 3D), suggesting that SA can suppress RANKL-induced NFATc1 expression. To further confirm that SA inhibited NFATc1 expression, we examined various concentrations and demonstrated that SA suppressed NFATc1 expression in dose dependent manner (Fig. 3D). Taken together, our results indicate that SA suppresses RANKL-induced NFATc1 expression in osteoclastogenesis and thus inhibits RANKL signaling pathway.

3.7. Therapeutic effects of SA on Ti particle-induced osteoclastic bone resorption in vivo

The effect of SA on in vivo bone lysis was examined in a murine calvaria model. Histological analysis showed that an intense inflammatory infiltrate with associated osteolysis after the implantation of Ti particles on mouse calvaria. Fibrous tissue laden with Ti particles and osteolysis were clearly seen in H&E stained tissue sections. As shown in Fig. 4A, Ti particles injected without any subsequent intervention (Ti-PBS) induced pronounced bone resorption. According to the histomorphometric analysis the average bone area of Ti particle implanted mice was significantly rescued by the treatment with SA (Fig. 4B). To determine whether Ti particles induce osteoclastogenesis in the calvaria and whether SA suppresses osteolysis, the results of histological TRAP staining were analyzed. A typical TRAP staining experiment is shown in Fig. 4B, in which TRAP+ cells are seen to have accumulated along the bone-membrane interface in Ti particle implanted calvaria.

4. Discussion

Excessive bone resorption plays a critical role in pathologic bone diseases [29]. Thus, inhibiting osteoclast activity could be a promising choice in the treatment for osteoclast-related diseases. Presently, we examined the effect of SA on osteoclasts formation from both BMMs and raw264.7 cell ling. Osteoclasts derived from BMMs or raw264.7 cells under the activation of RANKL [30,31]. Our results showed that SA inhibited RANKL-induced osteoclastogenesis without cytotoxicity.

Osteoclasts derive from monocyte-macrophage lineages [32]. Mature osteoclasts are characterized by the specific phenotypic markers expression, such as TRAP, OSCAR, c-Src, and CtsK, as well as multinucleated cells and the capability of bone resorption [9]. Our research demonstrated that SA dose-dependently reduced RANKL-induced maker genes expression.

NF-κB signaling plays a critical role in RANKL-induced osteoclast formation and function [25]. The classical NF-κB signaling pathway involves the IKK complex activation, which phosphorylates IκBα and leads to degradation [26]. This present study demonstrated that SA inhibited phosphorylation and degradation of IκBα, resulting in decreased NF-κB transactivation. These results showed that inhibition of the NF-κB pathway is one of the mechanisms involved in the anti-osteoclastogenic effect of SA.

Previous research has reported that RANKL-activated MAPKs (JNK, ERK and p38) signaling was associated with osteoclastogenesis [9,12]. Specifically, ERK is known to induce c-Fos for osteoclastogenesis, and inhibition of ERK has been shown to decrease osteoclast formation [33]. Meanwhile, dominant-negative JNK prevents RANKL-induced osteoclastogenesis [19], while p38 is important in the early stages of osteoclast generation because it regulates the microphthalmia-associated transcription factor [34]. Our present study evaluated the effects of SA on MAPKs signaling pathway and found that SA inhibited the phosphorylation of ERK and JNK while had no significant inhibition on p38 signaling. These results indicated that phosphorylation of MAPKs (JNK/ERK) may contribute to the anti-osteoclastogenic effect of SA. In addition, in vitro results further verified the bone protective role of SA on osteolysis model, which was consistent with attenuated bone loss and reduced osteoclast numbers.

Taken together, this present study demonstrated that SA inhibited osteoclast formation and bone resorption in vitro. SA also reduced the RANKL-induced osteoclastic marker genes expression. Furthermore, SA attenuated RANKL-induced NF-κB and MAPKs (ERK, JNK) activation, thus suppressed NFATc1 expression. In addition, our in vitro results further verified the bone protective role of SA on osteolysis model. However, further investigation of SA on other cells within bone is still required.

Conflicts of interest

The authors have no conflicts of interest to declare.

Acknowledgments

None.

References

[1] G. Karsenty, E.F. Wagner, Reaching a genetic and molecular understanding of skeletal development, Dev. Cell 2 (2002) 389–406.
[2] G.A. Rodan, T.J. Martin, Therapeutic approaches to bone diseases, Science 289 (2000) 1508–1514.
[3] T. Suda, N. Takahashi, T.J. Martin, Modulation of osteoclast differentiation, Endocr. Rev. 13 (1992) 66–80.
[4] F. Arai, T. Miyamoto, O. Ohneda, T. Inada, T. Sudo, K. Brasel, T. Miyata, D.M. Anderson, T. Suda, Commitment and differentiation of osteoclast precursor cells by the sequential expression of c-Fms and receptor activator of nuclear factor κB (RANK) receptors, J. Exp. Med. 190 (1999) 1741–1754.
[5] D. Lacey, E. Timms, H.-L. Tan, M. Kelley, C. Dunstan, T. Burgess, R. Elliott, A. Colombero, G. Elliott, S. Scully, Osteoprotegerin ligand is a cytokine that regulates osteoclast differentiation and activation, Cell 93 (1998) 165–176.
[6] B.G. Darnay, B.B. Aggarwal, Signal transduction by tumour necrosis factor and tumour necrosis factor related ligands and their receptors, Ann. Rheum. Dis. 58 (1999) I2–I13.
[7] B.G. Darnay, V. Haridas, J. Ni, P.A. Moore, B.B. Aggarwal, Characterization of the intracellular domain of receptor activator of NF-κB (RANK) Interaction with tumor necrosis factor receptor-associated factors and activation of NF-κB and c-Jun N-terminal kinase, J. Biol. Chem. 273 (1998) 20551–20555.
[8] B.R. Wong, R. Josien, S.Y. Lee, M. Vologodskaia, R.M. Steinman, Y. Choi, The TRAF family of signal transducers mediates NF-κB activation by the TRANCE receptor, J. Biol. Chem. 273 (1998) 28355–28359.
[9] W.J. Boyle, W.S. Simonet, D.L. Lacey, Osteoclast differentiation and activation, Nature 423 (2003) 337–342.
[10] U.H. Lerner, New molecules in the tumor necrosis factor ligand and receptor superfamilies with importance for physiological and pathological bone resorption, Crit. Rev. Oral Biol. Med. 15 (2004) 64–81.
[11] S.L. Teitelbaum, F.P. Ross, Genetic regulation of osteoclast development and function, Nat. Rev. Genet. 4 (2003) 638–649.
[12] Z.H. Lee, H.-H. Kim, Signal transduction by receptor activator of nuclear factor kappa B in osteoclasts, Biochem. Biophys. Res. Commun. 305 (2003) 211–214.
[13] H. Takayanagi, S. Kim, T. Koga, H. Nishina, M. Isshiki, H. Yoshida, A. Saiura, M. Isobe, T. Yokochi, J.-i. Inoue, Induction and activation of the transcription factor NFATc1 (NFAT2) integrate RANKL signaling in terminal differentiation of osteoclasts, Dev. Cell 3 (2002) 889–901.
[14] T. Koga, M. Inui, K. Inoue, S. Kim, A. Suematsu, E. Kobayashi, T. Iwata, H. Ohnishi, T. Matozaki, T. Kodama, Costimulatory signals mediated by the ITAM motif cooperate with RANKL for bone homeostasis, Nature 428 (2004) 758–763.
[15] A. Mócsai, M.B. Humphrey, J.A. Van Ziffle, Y. Hu, A. Burghardt, S.C. Spusta, S. Majumdar, L.L. Lanier, C.A. Lowell, M.C. Nakamura, The immunomodulatory adapter proteins DAP12 and Fc receptor γ-chain (FcRγ) regulate development of functional osteoclasts through the Syk tyrosine kinase, Proc. Nat. Acad. Sci. U.S.A. 101 (2004) 6158–6163.
[16] Y. Kiso, M. Tohkin, H. Hikino, Y. Ikeya, H. Taguchi, Mechanism of antihepatotoxic activity of wuweizisu C and gomisin A, Planta Med. 51 (1985) 331–334.
[17] M. Kogawa, K. Hisatake, G.J. Atkins, D.M. Findlay, Y. Enoki, T. Sato, P.C. Gray, Y. Kanesaki-Yatsuka, P.H. Anderson, S. Wada, The Paired-box homeodomain transcription factor Pax6 binds to the upstream region of the TRAP gene promoter and suppresses receptor activator of NF-κB Ligand (RANKL)-induced osteoclast differentiation, J. Biol. Chem. 288 (2013) 31299–31312.
[18] W. Zou, T. Izawa, T. Zhu, J. Chappel, K. Otero, S.J. Monkley, D.R. Critchley, B.G. Petrich, A. Morozov, M.H. Ginsberg, Talin1 and Rap1 are critical for osteoclast function, Mol. Cell. Biol. 33 (2013) 830–844.
[19] F. Ikeda, R. Nishimura, T. Matsubara, S. Tanaka, J.-i. Inoue, S.V. Reddy, K. Hata, K. Yamashita, T. Hiraga, T. Watanabe, Critical roles of c-Jun signaling in regulation of NFAT family and RANKL-regulated osteoclast differentiation, J. Clin. Investig. 114 (2004) 475–484.
[20] T.J. Weber, L.M. Markillie, Regulation of activator protein-1 by 8-iso-prostaglandin E2 in a thromboxane A2 receptor-dependent and-independent manner, Mol. Pharmacol. 63 (2003) 1075–1081.
[21] D.-K. Shin, M.-H. Kim, S.-H. Lee, T.-H. Kim, S.-Y. Kim, Inhibitory effects of luteolin on titanium particle-induced osteolysis in a mouse model, Acta Biomater. 8 (2012) 3524–3531.

[22] N. Soysa, N. Alles, NF-κB functions in osteoclasts, Biochem. Biophys. Res. Commun. 378 (2009) 1–5.
[23] K.M. Ghosh Sankar, Missing pieces in the NF-kappaB puzzle, Cell 109 (2002) S81–S96.
[24] A.E. Grigoriadis, Z.-Q. Wang, M.G. Cecchini, W. Hofstetter, R. Felix, H.A. Fleisch, E.F. Wagner, c-Fos: a key regulator of osteoclast-macrophage lineage determination and bone remodeling, Science 266 (1994) 443–448.
[25] Q. Zhao, X. Wang, Y. Liu, A. He, R. Jia, NFATc1: functions in osteoclasts, Int. J. Biochem. Cell Biol. 42 (2010) 576–579.
[26] M. Asagiri, H. Takayanagi, The molecular understanding of osteoclast differentiation, Bone 40 (2007) 251–264.
[27] M. Asagiri, K. Sato, T. Usami, S. Ochi, H. Nishina, H. Yoshida, I. Morita, E.F. Wagner, T.W. Mak, E. Serfling, Autoamplification of NFATc1 expression determines its essential role in bone homeostasis, J. Exp. Med. 202 (2005) 1261–1269.
[28] H. Takayanagi, Osteoimmunology: shared mechanisms and crosstalk between the immune and bone systems, Nat. Rev. Immunol. 7 (2007) 292–304.
[29] S.R. Cummings, L.J. Melton, Epidemiology and outcomes of osteoporotic fractures, Lancet 359 (2002) 1761–1767.
[30] T. Suda, N. Takahashi, N. Udagawa, E. Jimi, M.T. Gillespie, T.J. Martin, Modulation of osteoclast differentiation and function by the new members of the tumor necrosis factor receptor and ligand families, Endocr. Rev. 20 (1999) 345–357.
[31] S.L. Teitelbaum, RANKing c-Jun in osteoclast development, J. Clin. Investig. 114 (2004) 463–465.
[32] S.G.-K. Mohamed, E. Sugiyama, K. Shinoda, H. Taki, H. Hounoki, H.O. Abdel-Aziz, M. Maruyama, M. Kobayashi, H. Ogawa, T. Miyahara, Interleukin-10 inhibits RANKL-mediated expression of NFATc1 in part via suppression of c-Fos and c-Jun in RAW264. 7 cells and mouse bone marrow cells, Bone 41 (2007) 592–602.
[33] E. Ang, Q. Liu, M. Qi, H.G. Liu, X. Yang, H. Chen, M.H. Zheng, J. Xu, Mangiferin attenuates osteoclastogenesis, bone resorption, and RANKL-induced activation of NF-κB and ERK, J. Cell. Biochem. 112 (2011) 89–97.
[34] M. Matsumoto, T. Sudo, T. Saito, H. Osada, M. Tsujimoto, Involvement of p38 mitogen-activated protein kinase signaling pathway in osteoclastogenesis mediated by receptor activator of NF-κB ligand RANKL, J. Biol. Chem. 275 (2000) 31155–31161.